Modeling and Simulation of Time-Correlation Properties of Spectrum Use in Cognitive Radio

Miguel López-Benítez and Fernando Casadevall
Department of Signal Theory and Communications
Universitat Politècnica de Catalunya (UPC)
Barcelona, Spain
Email: {miguel.lopez, ferranc}@tsc.upc.edu

***Abstract*—The development of the cognitive radio technology can enormously benefit from the availability of realistic and accurate spectrum occupancy models. Time-dimension models of spectrum use proposed in the literature so far are able to capture and reproduce essential temporal characteristics such as the mean occupancy level (duty cycle) and the statistical distribution of busy/idle-period lengths. However, more sophisticated aspects of spectrum use, such as time-correlation properties, have not been properly addressed yet. In this context, this paper studies and analyzes, based on field measurements of various radio technologies, the time-correlation properties of spectrum use. Appropriate models and simulation techniques are proposed in order to accurately capture and reproduce such features.**

I. Introduction

The recent emergence of Dynamic Spectrum Access (DSA) policies based on the Cognitive Radio (CR) technology [1] has been motivated by the spectrum underutilization resulting from inflexible and inefficient spectrum access policies, which has been demonstrated by many spectrum measurement campaigns [2]–[11]. The basic underlying principle of DSA/CR is to allow unlicensed users to access in an opportunistic and non-interfering manner some licensed bands temporarily unoccupied by licensed users. Unlicensed (secondary) CR terminals monitor the spectrum in order to detect spectrum gaps left unused by licensed (primary) users and opportunistically transmit. Secondary unlicensed transmissions are allowed according to this operating principle as long as they do not result in harmful interference to the licensees.

As a result of the opportunistic nature of the DSA/CR paradigm, the behavior and performance of a network of secondary CR nodes depends on the primary spectrum occupancy pattern. Realistically and accurately modeling such patterns becomes therefore essential and extremely useful in the domain of DSA/CR research. Models of spectrum use can be very helpful in a wide variety of applications, ranging from analytical studies to the design, dimensioning and performance evaluation of secondary networks, including the development of innovative simulation tools as well as novel DSA/CR techniques. The utility of such models, however, depends on their degree of realism. An accurate modeling of the primary system's spectral activity is therefore a key aspect for a reliable design and performance evaluation of DSA/CR techniques.

This paper addresses the problem of modeling spectrum occupancy in the time domain. From the point of view of a DSA/CR network, spectrum use can adequately be modeled by means of a Markov chain with two states, one indicating that the channel is busy (i.e., used by a primary user and therefore not available for opportunistic access) and the other one indicating that it is idle (i.e., available for secondary use). Previous works based on empirical measurements have demonstrated the suitability of the Continuous-Time Semi-Markov Chain (CTSMC) model, where the busy/idle state holding times follow certain specified distributions [12]–[14].

The CTSMC model is able to capture and reproduce the statistical distribution of busy/idle-period lengths as well as the mean channel occupancy level in terms of the duty cycle (i.e., the probability/fraction of time that the channel is busy), which in turn depends on the mean value of the busy/idle-period distributions. Nevertheless, previous studies [14] have indicated that in some cases the lengths of the busy/idle periods in a given frequency band can be correlated, a feature that the CTSMC model cannot reproduce. A modeling approach based on the aggregation and superposition of the realizations of several CTSMC processes was proposed in [15]. Although such simple model was shown to be able to qualitatively reproduce correlations between consecutive idle-period lengths, it suffers from some practical limitations. The resulting correlation depends on the number of aggregated processes as well as their distributions, and by suitable parameter selection various correlations can be reproduced. However, if a particular correlation level needs to be reproduced, the number of processes to be aggregated and the distribution parameters cannot easily be determined, making necessary the use of simulations, which complicates the configuration of the model and hence its application. Therefore, there is a clear need for simple primary user activity models featuring correlated busy/idle periods. In this context, and based on field measurements of various radio technologies, this work explores the autocorrelation properties not only of idle periods but also of busy ones, as well as the correlation properties of consecutive busy/idle periods. Based on the observed correlation properties, adequate empirical models are developed. Moreover, a simulation method is proposed, which is able to reproduce the observed correlation properties between consecutive busy/idle, busy/busy or idle/idle periods along with any specified statistical distributions for both busy and idle periods.

II. Measurement Setup and Methodology

The measurement equipment used in this work (see Figure 1) relies on a spectrum analyzer configuration where some external devices have been added to improve the detection capabilities and therefore the accuracy and reliability of measurements. The setup is composed of two broadband discone-type antennas covering the frequency range from 75 to 7075 MHz, a Single-Pole Double-Throw (SPDT) switch to select the desired antenna, several filters to remove undesired overloading (FM) and out-of-band signals, a low-noise pre-amplifier to enhance the overall sensitivity and thus the ability to detect

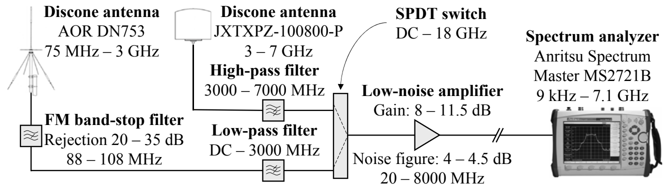

Fig. 1. Measurement setup employed in this study.

weak signals, and a high performance spectrum analyzer to record the spectral activity. A more detailed description of the measurement setup design and configuration as well as the methodological procedures considered can be found in [16].

The measurement equipment of Figure 1 was employed to monitor the activity of several spectrum bands, namely TETRA uplink (410–420 MHz) and downlink (420–430 MHz), E-GSM 900 uplink (880–915 MHz) and downlink (925–960 MHz), DCS 1800 uplink (1710–1785 MHz) and downlink (1805–1880 MHz), DECT (1880–1900 MHz), and ISM (2400–2500 MHz). Each band was measured for a time period of 7 days, beginning on Monday midnight and ending on Sunday midnight. The captured data were used to extract the binary channel occupancy patterns by classifying power samples as either busy channels or idle ones based on the energy detection method [17]. Based on the resulting binary channel occupancy sequences, the lengths of busy/idle periods were extracted and their correlation properties were exhaustively analyzed. Although this work does not present results for all the considered spectrum bands, the proposed modeling approach has been developed and validated based on channels from all the measured bands.

III. Correlation Metrics

The correlation properties of busy/idle periods are quantified and analyzed in this work by means of the Pearson's product-moment correlation coefficient ρ, the Kendall's rank correlation coefficient τ, and the Spearman's rank correlation coefficient ρ_s, which are defined as [18]:

$$\rho(T_i, T_j) = \frac{\mathbb{C}\{T_i, T_j\}}{\sqrt{\mathbb{V}\{T_i\}\mathbb{V}\{T_j\}}} \quad (1)$$

$$= \frac{\mathbb{E}\{(T_i - \mathbb{E}\{T_i\})(T_j - \mathbb{E}\{T_j\})\}}{\sqrt{\mathbb{V}\{T_i\}\mathbb{V}\{T_j\}}} \quad (2)$$

$$\tau(T_i, T_j) = \text{Prob}\left((T_i' - T_j')(T_i'' - T_j'') > 0\right) - \text{Prob}\left((T_i' - T_j')(T_i'' - T_j'') < 0\right) \quad (3)$$

$$= 2\,\text{Prob}\left((T_i' - T_j')(T_i'' - T_j'') > 0\right) - 1 \quad (4)$$

$$\rho_s(T_i, T_j) = \rho(F_i(T_i), F_j(T_j)) \quad (5)$$

where T_i and T_j represent the busy/idle period lengths with Cumulative Distribution Functions (CDF) $F_i(T_i)$ and $F_j(T_j)$, (T_i', T_j') and (T_i'', T_j'') are two random observations of T_i and T_j, and $\mathbb{E}\{\cdot\}$, $\mathbb{V}\{\cdot\}$, and $\mathbb{C}\{\cdot\}$ denote their expected value (mean), variance, and covariance, respectively. If the state space of a primary radio channel is denoted as $\mathbb{S} = \{s_i\}_{i=0,1}$, with s_0 being the idle state and s_1 being the busy state, then the previous correlation coefficients represent the autocorrelation of idle periods when $T_i = T_j = T_0$, the autocorrelation of busy periods when $T_i = T_j = T_1$, and the correlation between consecutive busy/idle periods when $T_i \neq T_j$, $i, j \in \{0, 1\}$.

Based on K empirical samples of the period lengths T_i and T_j, the previous correlation metrics can be estimated as:

$$\widehat{\rho}(T_i, T_j) = \frac{\sum_{k=1}^{K} T_i^k T_j^k - K\widetilde{m}_i\widetilde{m}_j}{(K-1)\sqrt{\widetilde{v}_i\widetilde{v}_j}} \quad (6)$$

$$\widehat{\tau}(T_i, T_j) = \frac{\mathcal{C} - \mathcal{D}}{\mathcal{C} + \mathcal{D}} = \frac{\mathcal{S}}{\binom{K}{2}} = \frac{2\mathcal{S}}{K(K-1)} \quad (7)$$

$$\widehat{\rho}_s(T_i, T_j) = \widehat{\rho}(F_i(T_i), F_j(T_j)) \quad (8)$$

where T_i^k/T_j^k $(k = 1, 2, \ldots, K)$, $\widetilde{m}_i/\widetilde{m}_j$ and $\widetilde{v}_i/\widetilde{v}_j$ represent the k-th value, the sample mean and the sample variance of T_i/T_j, respectively, and $\mathcal{S} = \mathcal{C} - \mathcal{D}$ is the difference between the number $\mathcal{C}$ of concordant pairs $((T_i' - T_j')(T_i'' - T_j'') > 0)$ and the number $\mathcal{D}$ of discordant pairs $((T_i' - T_j')(T_i'' - T_j'') < 0)$ observed in the sample set.

The above mentioned correlation coefficients have some similarities. All of them take values within the interval $[-1, +1]$. If both random variables T_i and T_j increase or decrease together, the correlation coefficients are positive. However, if one variable increases as the other decreases, then the correlation coefficients are negative. If the variables are independent, the correlation coefficients are zero (or approximately zero), but the converse is not true in general. There are, however, some important differences. First, ρ is only sensitive to linear dependence relations between random variables. Thus, if the association between two random variables is purely non-linear, then $\rho = 0$ even though they are not independent. On the other hand, τ and ρ_s are sensitive and can detect some non-linear associations between variables. Moreover, ρ has the unfortunate property of being sensitive (not invariant) under non-linear transformations of the random variables. However, τ and ρ_s are invariant under monotone transformations. Thus, given two random variables with correlation coefficients ρ, τ and ρ_s, a transformation of the variables could (and usually does) change the value of ρ, but it will not affect the values of τ and ρ_s under strictly monotone transformations.

IV. Correlation Properties of Spectrum Use

A. Correlation between Busy and Idle Periods

The correlation between busy/idle periods was evaluated for all channels within each measured band as a function of various parameters such as the channel duty cycle as well as the mean busy/idle period duration. The obtained results indicated that there is no clear relation between the observed correlation coefficients and these parameters. However, consecutive busy/idle periods frequently showed non-zero correlations, meaning that they are not completely independent and, as such, need to be modeled as correlated random variables.

Figure 2 shows the empirical Probability Density Function (PDF) of the considered correlation coefficients for the channels measured within the DCS 1800 downlink (DL) band, which constitutes a representative example of the results obtained for other spectrum bands. As it can be appreciated, the values obtained for the three considered correlation coefficients are frequently close to zero, meaning that consecutive busy/idle periods are not tightly correlated. However, the correlation values are mostly non-zero and, in some particular cases, they indicate noticeable correlation levels. An accurate and realistic model of spectrum use should therefore take this feature into account. In order to characterize the correlation

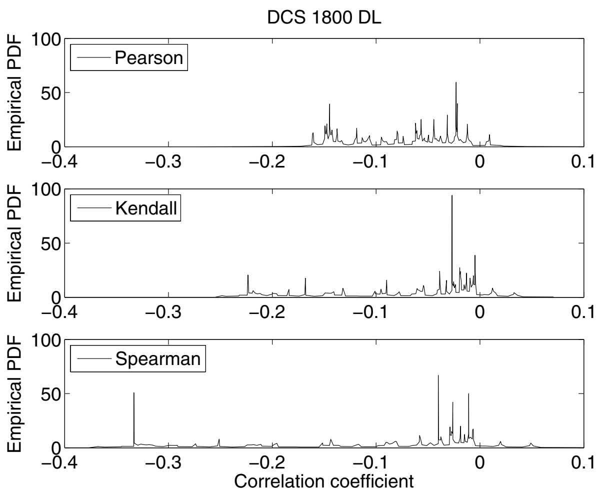

Fig. 2. Empirical PDF of the correlation coefficients for DCS 1800 DL.

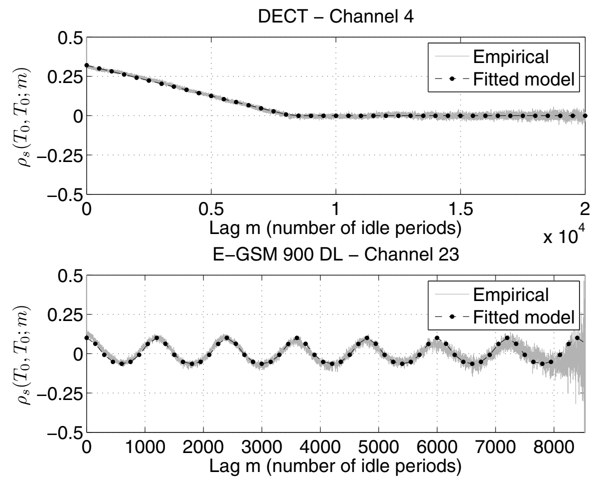

Fig. 3. Spearman's autocorrelation functions of idle periods.

TABLE I
BUSY/IDLE CORRELATION COEFFICIENTS FOR THE MEASURED BANDS.

Band	Metric	(min; mean; max)
TETRA DL	$\rho(T_0, T_1)$	(−0.19; −0.03; 0.14)
	$\tau(T_0, T_1)$	(−0.36; −0.03; 0.13)
	$\rho_s(T_0, T_1)$	(−0.53; −0.04; 0.20)
E-GSM 900 DL	$\rho(T_0, T_1)$	(−0.17; −0.04; 0.01)
	$\tau(T_0, T_1)$	(−0.27; −0.16; 0.01)
	$\rho_s(T_0, T_1)$	(−0.39; −0.24; 0.01)
DCS 1800 DL	$\rho(T_0, T_1)$	(−0.27; −0.07; 0.24)
	$\tau(T_0, T_1)$	(−0.47; −0.08; 0.07)
	$\rho_s(T_0, T_1)$	(−0.64; −0.12; 0.11)
DECT	$\rho(T_0, T_1)$	(−0.15; −0.10; −0.05)
	$\tau(T_0, T_1)$	(−0.13; −0.09; −0.04)
	$\rho_s(T_0, T_1)$	(−0.20; −0.14; −0.06)
ISM	$\rho(T_0, T_1)$	(−0.10; −0.05; −0.02)
	$\tau(T_0, T_1)$	(−0.04; −0.01; 0.02)
	$\rho_s(T_0, T_1)$	(−0.05; −0.02; 0.03)

properties of busy/idle periods, Table I shows the correlation coefficients observed for some selected spectrum bands.

It is worth noting in Figure 2 and Table I that the correlation coefficients normally take negative values, meaning that when the length of a busy period increases, the length of the next idle period tends to decrease and vice versa. This can be explained by the fact that when the channel load increases, then the fraction of time that it remains in use increases and, as a result, the duration of busy periods increases while idle periods become shorter. On the other hand, the opposite behavior is observed when the channel load decreases (i.e., the length of busy periods decreases and idle periods become longer).

B. Autocorrelation of Busy and Idle Periods

The correlation between the sequence of periods of the same type (either busy or idle) of a channel and a shifted version of itself (i.e., the autocorrelation) was also evaluated based on the considered correlation metrics as a function of the distance (lag) between them. Two different autocorrelation behaviors were empirically observed, namely one periodic and another non-periodic. This is illustrated in Figure 3, which shows some examples of the autocorrelation function of idle periods as a function of the lag number, m, based on the Spearman's correlation coefficient, i.e. $\rho_s(T_0, T_0; m)$. Similar trends were observed for busy periods and other correlation metrics.

For channels with non-periodic autocorrelation functions (upper part of Figure 3), the correlation coefficient takes its maximum value ρ_s^{max} at $m = 1$ and decreases linearly with m until $m = M$, beyond which the correlation is approximately zero. This behavior can adequately be modeled as:

$$\rho_s(T_i, T_i; m) = \begin{cases} 1, & m = 0 \\ \rho_s^{max}\left(\frac{M-m}{M-1}\right), & 1 \leq m \leq M \\ 0, & m > M \end{cases} \quad (9)$$

Based on results from field measurements, it was empirically observed that $\rho_s^{max} \in [0.1, 0.4]$ and $M \in [2000, 8000]$.

For channels with periodic autocorrelation functions (lower part of Figure 3) with period M, the correlation coefficient can be expressed as the summation of two bell-shaped exponential terms centered at lags $m = 1$ and $m = M+1$, with amplitudes A and widths σ:

$$\rho_s(T_i, T_i; m) = \begin{cases} 1, & m = 0 \\ \rho_s^{min} + Ae^{-\left(\frac{m-1}{\sigma}\right)^2} & \\ \quad + Ae^{-\left(\frac{m-M-1}{\sigma}\right)^2}, & 1 \leq m \leq M \end{cases} \quad (10)$$

where ρ_s^{min} is the minimum correlation. This behavior was frequently observed in cellular mobile communication systems (and some TETRA channels) where the experienced loads, and thus the busy/period lengths, show a relatively similar and periodic behavior every day. Based on results from field measurements, it was empirically observed that $\rho_s^{min} \approx -0.1$ in most cases, $A \in [0.2, 0.5]$, M corresponds to the average number of lags equivalent to 24 hours, and $\sigma \approx M/4$.

As it can clearly be appreciated in Figure 3, the models of equations 9 and 10 are able to accurately describe the time-domain autocorrelation properties of spectrum use empirically observed in real systems.

V. Random Variate Generation Principles

This section reviews some results from the theory of random variate generation, which will be used in the definition of the simulation technique proposed in Section VI in order to reproduce the time-correlation properties of spectrum use.

A. The Inversion Method

The inversion method [18, p. 28] can be used to generate random variates with any arbitrary distribution. This method is based on the following property. Let $F(\cdot)$ be a continuous CDF on $\mathbb{R}$ with inverse CDF given by $F^{-1}(\cdot)$. If U is a uniform random variable within the interval $[0,1]$, then the CDF of $F^{-1}(U)$ is $F(\cdot)$. Moreover, if X is a random variable with CDF $F(\cdot)$, then $F(X)$ is uniformly distributed on $[0,1]$. Based on this property, any distribution $F(\cdot)$ can be generated based on random variates with uniform or any other distributions.

B. Generation of Correlated Random Variates

If Y and Z are independent and identically distributed (iid) random variables, and a new random variable X is defined as:

$$X = \rho_0 \, Y + \sqrt{1-\rho_0^2}\, Z \tag{11}$$

with $\rho_0 \in [-1,+1]$, then X and Y have a Pearson's correlation coefficient $\rho(X,Y) = \rho_0$ [18, p. 567]. This property, which can be verified from equation 1, can be used to generate random variates with a specified Pearson's correlation coefficient.

It is worth mentioning that the normal distribution is one of the few distributions that is stable, meaning that a linear combination of two independent variables of such distribution also has the same distribution, up to the location and scale parameters. Therefore, if Y and Z are normally distributed, then X is also normally distributed. Moreover, if Y and Z are standard (zero-mean, unit-variance) normal random variables, then X is also a standard normal random variable.

A sequence $X = x_1, x_2, \ldots, x_M$ of M standard normal random values with specified Pearson's autocorrelation function $\rho(X,X;m)$ can be generated based on the property:

$$\mathcal{F}\left\{\rho(X,X;m)\right\} = \left|\mathcal{F}\left\{X\right\}\right|^2 \tag{12}$$

derived from the Wiener-Khinchin theorem, where $\mathcal{F}\{\cdot\}$ denotes the Fourier transform. Subjecting a standard Gaussian process to a linear operation (including filtering) yields another standard Gaussian process with a different autocorrelation function. Thus, an appropriate filter (derived from equation 12) can be used to induce correlation on an uncorrelated Gaussian process. Concretely, if $Y = y_1, y_2, \ldots, y_M$ is a sequence of iid complex standard normal random values, then [19]:

$$X = \mathrm{Re}\left\{\mathcal{F}^{-1}\left\{Y \odot \sqrt{\left|\mathcal{F}\left\{\rho(X,X;m)\right\}\right|}\right\}\right\} \tag{13}$$

is a sequence $X = x_1, x_2, \ldots, x_M$ of standard normal random values with Pearson's autocorrelation function $\rho(X,X;m)$, where $\odot$ stands for Hadamard's element-wise multiplication.

C. Relation among Correlation Metrics

For normally distributed random variables X and Y, the correlation metrics defined in equations 1–5 are related as [20]:

$$\rho(X,Y) = \sin\left(\frac{\pi}{2}\tau(X,Y)\right) = 2\sin\left(\frac{\pi}{6}\rho_s(X,Y)\right) \tag{14}$$

Equation 14 holds if X and Y are normally distributed. If a monotone transformation is applied to X and/or Y, $\tau(X,Y)$ and $\rho_s(X,Y)$ will remain unchanged but $\rho(X,Y)$ might not.

VI. Simulation of Correlation Properties

A. Simulation Method

A simulation method is proposed in order to reproduce any arbitrary distribution of busy/idle period lengths along with the correlation properties of spectrum use observed in Section IV (see Algorithm 1). The proposed algorithm requires as input information the CDF of idle and busy periods, denoted as $F_0(\cdot)$ and $F_1(\cdot)$ respectively, the Kendall or Spearman correlation coefficient between busy/idle periods, denoted as $\tau(T_0,T_1)$ and $\rho_s(T_0,T_1)$ respectively, as well as the autocorrelation function (periodic or non-periodic) of idle periods in terms of the Kendall or Spearman correlation coefficients as a function of the lag number m, i.e. $\tau(T_0,T_0;m)$ or $\rho_s(T_0,T_0;m)$ respectively. Notice that the desired correlations to be reproduced need to be specified in terms of the Kendall or Spearman metrics since the algorithm involves some transformations of random variables that would change any specified Pearson's correlation value. The same algorithm can be used to reproduce the autocorrelation properties of busy periods, i.e. $\tau(T_1,T_1;m)$ or $\rho_s(T_1,T_1;m)$, instead of idle ones, if desired. However, idle periods represent the real spectrum opportunities for secondary users and modeling their autocorrelation properties results therefore more convenient. The proposed algorithm outputs sequences of period durations for idle, T_0, and busy, T_1, periods, in blocks of M values.

For periodic idle autocorrelation functions, M corresponds to the function's period and determines the periodicity with which the process is repeated. For non-periodic idle autocorrelation functions, M represents the lag number beyond which autocorrelation is negligible. In such a case, after generating a sequence of M period lengths, a new one is generated based on different (independent) random variates.

First of all, the correlation properties specified in terms of the Kendall or Spearman metrics are converted to their Pearson counterpart based on equation 14 (lines 1 and 2). Afterwards, and for every block of M values, a sequence ϑ of M iid complex standard normal variates is generated (line 4) and converted, based on equation 13, into a sequence ξ_0 (line 5) of standard normal variates with autocorrelation function $\rho(T_0,T_0;m)$. A sequence χ of M iid standard normal variates is generated (line 6) in order to produce, based on equation 11, a sequence ξ_1 (line 7) that has a correlation $\rho(T_0,T_1)$ with ξ_0. Since ξ_0 and ξ_1 are standard normal variates, $\Phi(\xi_0)$ and $\Phi(\xi_1)$, where $\Phi(x) = \frac{1}{2}[1+\mathrm{erf}\left(x/\sqrt{2}\right)]$ is the standard normal CDF, are uniformly distributed. Thus, by the inversion principle, the transformations of lines 8 and 9 produce sequences T_0 and T_1 of M period lengths with the desired CDFs. Moreover, since ξ_0 and ξ_1 are normally distributed, the desired Kendall and Spearman correlations hold between them as inferred from equation 14. As a result, the monotone transformations of lines 8 and 9 preserve such correlations on T_0 and T_1.

B. Validation

The proposed method was employed to generate sequences of idle/busy periods following generalized Pareto distributions with locations $\mu_0/\mu_1 = 3.5780/3.5150$ s, scales $\lambda_0/\lambda_1 = 10.9356/2.6240$ and shapes $\alpha_0/\alpha_1 = 0.1784/0.1884$ (these values were extracted from observations of empirical measurements). The algorithm was configured in order to reproduce $\rho_s(T_0,T_1) = -0.3$ with both non-periodic ($\rho_s^{max} = 0.25$, $M = 3000$) and periodic ($\rho_s^{min} = -0.1$, $A = 0.4$, $M = 1000$,

Algorithm 1 Proposed simulation method

Input: $F_0(\cdot)$, $F_1(\cdot)$, $\tau(T_0, T_1)$ or $\rho_s(T_0, T_1)$, $\tau(T_0, T_0; m)$ or $\rho_s(T_0, T_0; m)$
Output: T_0, T_1

$\rho(T_0, T_1) \leftarrow f\left(\{\tau(T_0, T_1) \,|\, \rho_s(T_0, T_1)\}\right)$
$\rho(T_0, T_0; m) \leftarrow f\left(\{\tau(T_0, T_0; m) \,|\, \rho_s(T_0, T_0; m)\}\right)$
for every block of M values **do**
  Generate $\vartheta = \vartheta_1, \vartheta_2, \ldots, \vartheta_M \sim \mathcal{CN}(0, 1)$
  $\xi_0 \leftarrow \mathrm{Re}\left\{\mathcal{F}^{-1}\{\vartheta \odot \sqrt{|\mathcal{F}\{\rho(T_0, T_0; m)\}|}\}\right\}$
  Generate $\chi = \chi_1, \chi_2, \ldots, \chi_M \sim \mathcal{N}(0, 1)$
  $\xi_1 \leftarrow \rho(T_0, T_1) \cdot \xi_0 + \sqrt{1 - [\rho(T_0, T_1)]^2} \cdot \chi$
  $T_0 \leftarrow F_0^{-1}\left(\Phi\left(\xi_0\right)\right)$
  $T_1 \leftarrow F_1^{-1}\left(\Phi\left(\xi_1\right)\right)$
end for

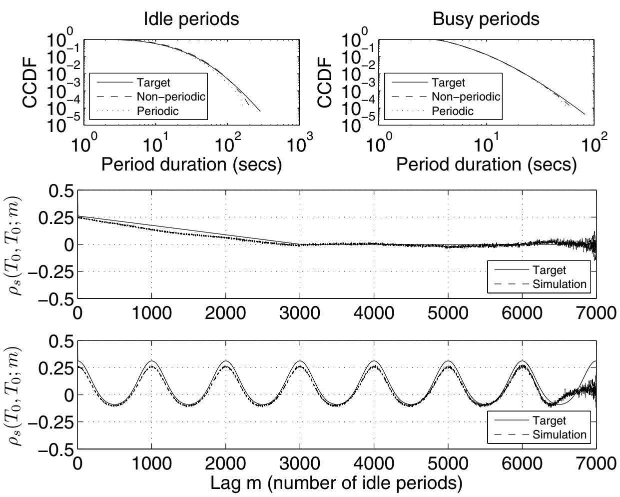

Fig. 4. Validation of the proposed simulation method.

$\sigma = M/4 = 250$) idle autocorrelation functions. Figure 4 shows the results obtained by averaging 10 simulations ($\rho_s(T_0, T_1) \approx -0.29$). As it can clearly be appreciated, the proposed method is able to accurately reproduce not only the specified statistical distributions for both busy and idle periods (shown in Figure 4 in terms of the complementary CDF), but also the desired time-correlation properties of spectrum use.

VII. Conclusions

An accurate and realistic modeling of the spectral activity of primary systems is a key aspect in the design and performance evaluation of DSA/CR systems. Existing time-dimension models of spectrum use are able to capture and reproduce basic temporal characteristics such as duty cycle and statistical distribution of busy/idle periods. However, more sophisticated aspects such as time-correlation properties have not been properly addressed. This paper has studied and analyzed, based on field measurements of various bands, the time-correlation properties of spectrum use, proposing adequate models and a simulation technique to accurately capture and reproduce such features. The obtained results demonstrate that the proposed models and simulation method are able to accurately reproduce not only any arbitrary statistical distributions for both busy and idle periods but also the time-correlation properties of spectrum use empirically observed in real systems.

Acknowledgements

This work was supported by the European Commission in the framework of the FP7 FARAMIR Project (Ref. ICT-248351) and the Spanish Research Council under research project ARCO (Ref. TEC2010-15198). The support from the Spanish Ministry of Science and Innovation (MICINN) under FPU grant AP2006-848 is hereby acknowledged.

References

[1] I. F. Akyildiz, W.-Y. Lee, M. C. Vuran, and S. Mohanty, “NeXt generation/dynamic spectrum access/cognitive radio wireless networks: a survey,” *Computer Networks*, vol. 50, no. 13, pp. 2127–2159, Sep. 2006.

[2] M. A. McHenry *et al.*, “Spectrum occupancy measurements,” Shared Spectrum Company, Tech. Rep., Jan 2004 - Aug 2005.

[3] A. Petrin and P. G. Steffes, “Analysis and comparison of spectrum measurements performed in urban and rural areas to determine the total amount of spectrum usage,” in *Proc. Int’l. Symp. on Advanced Radio Technologies (ISART 2005)*, Mar. 2005, pp. 9–12.

[4] R. I. C. Chiang, G. B. Rowe, and K. W. Sowerby, “A quantitative analysis of spectral occupancy measurements for cognitive radio,” in *Proc. IEEE 65th Vehicular Tech. Conf. (VTC 2007 Spring)*, Apr. 2007, pp. 3016–3020.

[5] M. Wellens, J. Wu, and P. Mähönen, “Evaluation of spectrum occupancy in indoor and outdoor scenario in the context of cognitive radio,” in *Proc. Second Int’l. Conf. on Cognitive Radio Oriented Wireless Networks and Comms. (CrownCom 2007)*, Aug. 2007, pp. 1–8.

[6] M. H. Islam *et al.*, “Spectrum survey in Singapore: Occupancy measurements and analyses,” in *Proc. 3rd Int’l. Conf. on Cognitive Radio Oriented Wireless Networks and Comms. (CrownCom 2008)*, May 2008, pp. 1–7.

[7] R. B. Bacchus, A. J. Fertner, C. S. Hood, and D. A. Roberson, “Long-term, wide-band spectral monitoring in support of dynamic spectrum access networks at the IIT spectrum observatory,” in *Proc. 3rd IEEE Int’l. Symp. on New Frontiers in Dynamic Spectrum Access Networks (DySPAN 2008)*, Oct. 2008, pp. 1–10.

[8] M. López-Benítez, F. Casadevall, A. Umbert, J. Pérez-Romero, J. Palicot, C. Moy, and R. Hachemani, “Spectral occupation measurements and blind standard recognition sensor for cognitive radio networks,” in *Proc. 4th Int’l. Conf. on Cognitive Radio Oriented Wireless Networks and Comms. (CrownCom 2009)*, Jun. 2009, pp. 1–9.

[9] K. A. Qaraqe, H. Celebi, A. Gorcin, A. El-Saigh, H. Arslan, and M. s. Alouini, “Empirical results for wideband multidimensional spectrum usage,” in *Proc. IEEE 20th Int’l. Symp. on Personal, Indoor and Mobile Radio Comms. (PIMRC 2009)*, Sep. 2009, pp. 1262–1266.

[10] R. Schiphorst and C. H. Slump, “Evaluation of spectrum occupancy in Amsterdam using mobile monitoring vehicles,” in *Proc. IEEE 71st Vehicular Tech. Conf. (VTC Spring 2010)*, May 2010, pp. 1–5.

[11] V. Valenta, R. Maršálek, G. Baudoin, M. Villegas, M. Suarez, and F. Robert, “Survey on spectrum utilization in Europe: Measurements, analyses and observations,” in *Proc. Fifth Int’l. Conf. on Cognitive Radio Oriented Wireless Networks & Comms. (CrownCom 2010)*, Jun. 2010, pp. 1–5.

[12] S. Geirhofer, L. Tong, and B. M. Sadler, “Dynamic spectrum access in the time domain: Modeling and exploiting white space,” *IEEE Comms. Magazine*, vol. 45, no. 5, pp. 66–72, May 2007.

[13] L. Stabellini, “Quantifying and modeling spectrum opportunities in a real wireless environment,” in *Proc. IEEE Wireless Comms. and Networking Conf. (WCNC 2010)*, Apr. 2010, pp. 1–6.

[14] M. Wellens, J. Riihijärvi, and P. Mähönen, “Empirical time and frequency domain models of spectrum use,” *Physical Comm.*, vol. 2, no. 1-2, pp. 10–32, Mar. 2009.

[15] ——, “Modelling primary system activity in dynamic spectrum access networks by aggregated ON/OFF-processes,” in *Proc. Fourth IEEE Workshop on Networking Technologies for Software Defined Radio Networks (SDR 2009)*, Jun. 2009, pp. 1–6.

[16] M. López-Benítez and F. Casadevall, “Methodological aspects of spectrum occupancy evaluation in the context of cognitive radio,” *European Transactions on Telecommunications, Special Issue on European Wireless 2009 Conference*, vol. 21, no. 8, pp. 680–693, Dec. 2010.

[17] H. Urkowitz, “Energy detection of unknown deterministic signals,” *Proceedings of the IEEE*, vol. 55, no. 4, pp. 523–531, Apr. 1967.

[18] L. Devroye, *Non-uniform random variate generation*. Springer-Verlag, 1986.

[19] G. N. Tavares and A. Petrolino, “On the generation of correlated Gaussian random variates by inverse DFT,” *IEEE Transactions on Communications*, vol. 59, no. 1, pp. 45–51, Jan. 2011.

[20] H. Hotelling and M. R. Pabst, “Rank correlation and tests of significance involving no assumption of normality,” *Annals of Mathematical Statistics*, vol. 7, no. 1, pp. 29–43, Mar. 1936.